A Hybrid RANS/LES Model for Predicting the Aerodynamics of Small City Vehicles

Mohammad Arafat[1], Izuan Amin Ishak[1,*], Muhammad Aidil Safwan Abdul Aziz[1], Andrew Soh Wee Shong[1], Tiong Woei Ting[1], Nur Rasyidah Roziman[1], Nur Amiza Mohd Hairul[1], Muhammad Aslam Ramli[1], Zainal Mukhriz Ahmad Puaat[1], Shahrizal Hafiz Shahmuddin[1], Razlin Abd Rashid[2]

[1] Faculty of Engineering Technology, Universiti Tun Hussein Onn Malaysia, Pagoh Campus, 84600, Muar, Johor, Malaysia
[2] Department of Chemical Engineering, The University of Manchester, Manchester, M13 9PL, United Kingdom

ABSTRACT

Electric city vehicles are vital for reducing pollution in urban areas due to their zero emissions and high energy efficiency, significantly improving air quality and reducing the carbon footprint. This study investigates the aerodynamic behavior of simplified city vehicle models using computational fluid dynamics (CFD) simulations based on Reynolds-Averaged Navier-Stokes (RANS) and Detached Eddy Simulation (DES) turbulence model. The models are tested at speeds of 10 m/s, 15 m/s, and 20 m/s, with a grid independence study to ensure reliable results. ANSYS Fluent is used for the simulations, comparing the results from RANS and hybrid RANS/LES or DDES in terms of aerodynamic forces and flow patterns around the vehicle. Results show that the drag coefficient (C_d) decreases with increasing speed for both RANS and DDES models. At 10 m/s, the drag coefficients are 0.541 for RANS and 0.524 for DDES, a 3.14% reduction. At 15 m/s, the drag coefficients are 0.539 for RANS and 0.518 for DDES, a 3.89% reduction. At 20 m/s, the drag coefficients are 0.538 for RANS and 0.514 for DDES, a 4.46% reduction. Flow visualizations show that DDES simulations capture more detailed and complex flow structures, particularly in the wake region, compared to the smoother RANS patterns. These findings are essential guidelines for optimizing vehicle design to enhance aerodynamic performance and contribute to the development of more efficient, environmentally friendly urban transportation solutions.

Keywords:
Aerodynamic; Computational Fluid Dynamics; electric city vehicles; hybrid turbulence models; pollution reduction

1. Introduction

Low-emission zones are recognized as crucial tools for cities striving to establish sustainable and environmentally friendly urban spaces by regulating emissions and promoting cleaner transportation options [1]. The inclusion of sustainable transport modes, such as electric vehicles and environmentally friendly hybrid vehicles, in public transport systems can help alleviate ecological environmental pressure, demonstrating the potential advantages of integrating green transportation options into city infrastructure [2]. Measures promoting environmentally friendly vehicles are shown

---

to benefit city users and transport operators, underscoring the positive impacts of embracing green transportation solutions in urban settings [3].

In the design stage of small city vehicles, conducting aerodynamic analysis is crucial for achieving optimal performance. Aerodynamics plays a significant role in enhancing handling, stability, and fuel efficiency of vehicles [4]. Utilizing continuous aerodynamic modelling methods can efficiently analyse aerodynamics at the design stage, enabling exploration of numerous design possibilities [5]. There are several approaches available for conducting aerodynamic analysis at the early design stage, including experiments, wind tunnel testing, and computational fluid dynamics (CFD) simulations. Each of these methods offers unique advantages in optimizing the aerodynamic performance of the vehicle.

Aerodynamic analysis plays a significant role in the design of vehicles, as it helps in identifying critical parameters and areas for improvement [6]. Utilizing CFD simulations has become a popular and effective tool in the automotive industry for aerodynamic design and analysis due to advancements in computational capabilities [7,8].

To accurately predict aerodynamic performance, the selection of an appropriate turbulence model is essential as it significantly impacts the results obtained from CFD simulations [9]. The Reynolds-averaged Navier–Stokes (RANS)-based CFD tools have been shown to provide accurate aerodynamic data for predicting overall vehicle performance with a high degree of accuracy [10], [11]. Furthermore, the use of RANS models like k-epsilon (k-ε) and k-omega (k-ω) has been common in aerodynamic simulation studies of vehicles using CFD [12]. However, several limitations have been identified when using RANS for accurately predicting the aerodynamics of vehicles. Studies have shown that the RANS approach often struggles to predict integral aerodynamic quantities such as lift, drag, and moment coefficients accurately [13]. Meanwhile, RANS has been found to face challenges in predicting critical aerodynamic aspects such as lift force accurately [14]. This limitation can be significant, especially in scenarios where precise lift predictions are essential for vehicle stability and performance evaluation. While RANS models are commonly used for predicting drag coefficients due to their influence on fuel consumption and emissions, they may not be as effective in capturing the full aerodynamic behavior of vehicles [15].

Detached Eddy Simulation (DES) is a computational fluid dynamics approach that combines the benefits of Reynolds-Averaged Navier-Stokes (RANS) and Large Eddy Simulation (LES) methods. Studies have shown that DES is particularly useful for predicting aerodynamic forces and flow structures in various applications, such as automotive aerodynamics [16], train aerodynamics [17-19], and high-speed train aerodynamics [20]. it has been noted that other models like the Detached-Eddy Simulation (DES) can offer better predictions in terms of aerodynamic forces and surface pressure compared to RANS [21]. DES has been recognized for its ability to predict aerodynamic characteristics and wake flows in scenarios involving high Reynolds numbers and massively separated flows [22]. The Delayed Detached-Eddy Simulation (DDES) approach, a variant of DES, has been employed to address the limitations of RANS models in simulating wake flows while avoiding the computational cost associated with full LES simulations [23].

It is noted that, in comparison to LES, DES offers significant computational savings for high Reynolds number flows by utilizing the moderate costs of RANS models in the boundary layer while still retaining some benefits of LES in separated regions [24]. Hybrid RANS-LES formulations, like DES, facilitate a transition from RANS to LES, providing enhanced accuracy over RANS models for automotive flows but at a higher computational cost [25]. DES has been observed to better replicate wind tunnel results within the margin of uncertainty compared to RANS in specific applications [26]. Knowing the capabilities of Detached-Eddy Simulation model, current study aims to investigate the effects of hybrid RANS/LES model for predicting the aerodynamics of small city vehicles. In addition,

a RANS simulation was carried out to compare the results with DDES. Current study focuses on aerodynamic load such drag and lift coefficient with flow around a simplified small city vehicle model.

The paper begins with a brief background, providing essential context and relevance of the study. It then details the methodology, outlining the vehicle model, computational domain and boundary conditions, and numerical techniques. This is followed by a mesh independence study, assessing how different mesh sizes impact the results and ensuring the accuracy of computational simulations. Finally, the paper presents the results and conclusions, summarizing key findings, interpreting their significance, and suggesting potential opportunities for future research.

2. Methodology
2.1 Geometry Modelling

In this study, a full-scale model of a simplified urban electric vehicle concept, inspired by the Podbike e-bike car model designed by Per Hassel Sørensen, was utilized. The Podbike is known for its compact and efficient design, blending the features of a bicycle and a car to create an innovative urban transport solution. Using Solidworks 3D modeling software, the model was designed, capturing the essential characteristics of the reference vehicle model. The model's dimensions are 2.3 m in length, 0.8 m in width, and 1.5 m in height shown in Figure 1, reflecting its compact nature and suitability for urban environments. Simplifying the model helps in focusing on the most critical aspects of the vehicle's performance while maintaining essential geometric and aerodynamic characteristics. This reduction in complexity ensures that the simulations can be performed more efficiently, saving both time and computational resources [27].
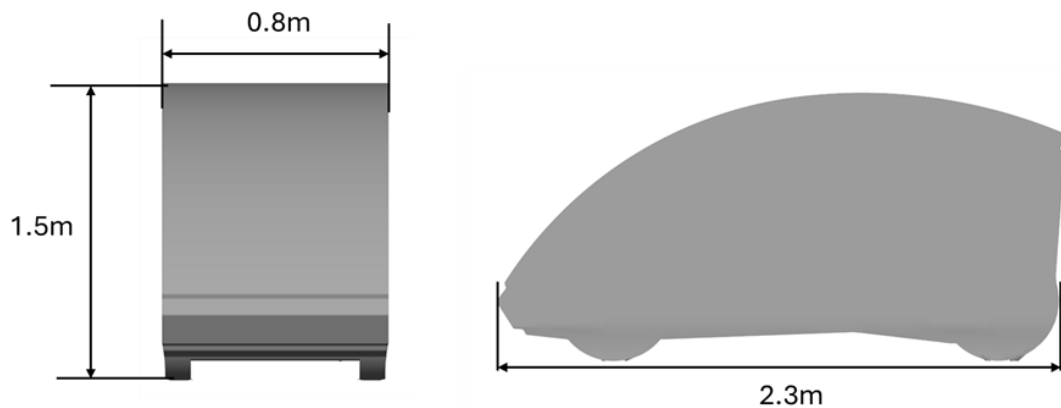

Fig. 1. Overall dimensions of the simplified city vehicle model designed in Solidworks software

2.2 Boundary Conditions and Simulation Setup

The computational domain was defined to encompass the full-scale vehicle model and extend sufficiently far in all directions to minimize the influence of boundary effects on the results [28]. Figure 2 depicts the computational domain used in current study.

The boundary conditions for the simulation were set up to ensure accurate and relevant results for urban driving scenarios. A uniform velocity inlet condition was applied at the upstream boundary with inlet velocities of 10 m/s, 15 m/s, and 20 m/s. At the downstream boundary, a pressure outlet condition allowed the flow to exit freely, set to atmospheric pressure to simulate an open environment [29]. The vehicle's surface was modelled as a no-slip wall, ensuring zero relative fluid

velocity to capture boundary layer development and drag forces accurately. The ground plane was also treated as a no-slip wall, with a steady ground condition as the interaction between the vehicle and the road surface are insignificant [30]. Additionally, the side and roof walls of the domain were treated as symmetry boundary conditions [31].
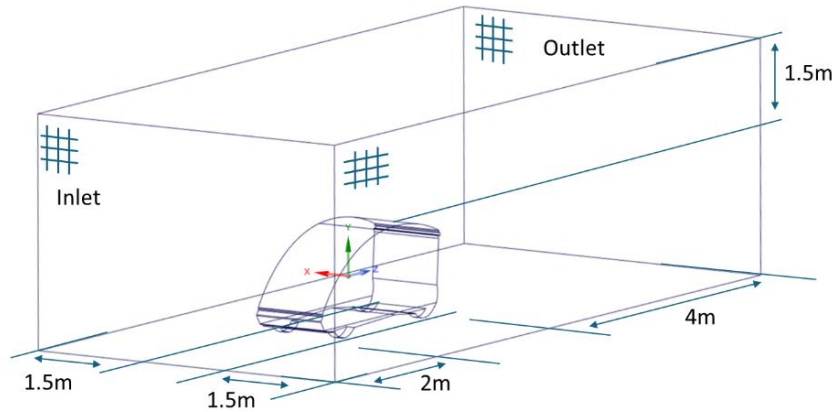

Fig. 2. Computation domain including the dimensions

To accurately capture the effects of turbulence in the flow around the simplified urban electric vehicle model, both Reynolds-Averaged Navier-Stokes (RANS) and Delayed Detached-Eddy Simulation (DDES) approaches were employed. Each method was chosen for its strengths in different aspects of the simulation. The details of the solver settings can be found in Table 1. For the steady-state simulations, the standard k-epsilon model was used with standard wall functions to treat the near-wall regions [32]. The SIMPLE algorithm was employed for pressure-velocity coupling, ensuring stable and convergent solutions [33]. Spatial discretization for gradients was performed using the Green-Gauss cell-based method. On the other hand, for the transient simulations, the Delayed Detached-Eddy Simulation (DDES) method was utilized, employing the k-omega SST model for better accuracy near the wall regions without any specific wall treatment. The transient simulations with a time steps size of 0.01 seconds. The SIMPLE algorithm was also used for pressure-velocity coupling. Steady RANS and transient DDES both simulations were conducted at the same inlet velocities of 10 m/s, 15 m/s, and 20 m/s.

Table 1
The turbulence modeling parameters for both Reynolds-Averaged Navier-Stokes (RANS) and Delayed Detached-Eddy Simulation (DDES) approaches used in the simulations

Parameter	RANS	Hybrid RANS/LES
Model	k-epsilon	DDES
Type	Standard	K-omega SST
Wall treatment	Standard wall functions	None
Solver type	Steady	Transient
Number of Iterations / Time Steps	1000	20 (100)
Timestep size	N/A	0.01 s
Pressure velocity coupling	SIMPLE	SIMPLE
Spatial discretization (Gradient)	Green-Gauss cell based	Green-Gauss cell based
Pressure	Second order	Second order
Momentum	Second order upwind	Bounded central differencing
Turbulent kinetic energy	First order upwind	Second order upwind
Turbulent dissipation rate	First order upwind	Second order upwind
Transient formulation	N/A	Bounded second order implicit

2.3 Mesh Independence Study

The computational domain surrounding the vehicle was meshed using a Cartesian grid to discretize the geometry into smaller elements in Ansys Advanced meshing module. The meshing strategy aimed to balance resolution and computational efficiency. A mesh independence study was conducted to assess the sensitivity of simulation results to changes in mesh resolution. This study involved systematically refining the mesh and analyzing how drag coefficient converge with increasing mesh refinement. The details meshing strategy with the associate meshing parameters can be found in Table 2.

Table 2
Meshing parameter descriptions

Parameters	Mesh 1	Mesh 2	Mesh 3
Number of elements	313794	675082	2811807
Total nodes	368874	763202	2946133
Element size (mm)	128	64	32
Face size (mm)	4	2	1
Drag Coefficient, C_d	0.568	0.546	0.541

Starting with a coarse mesh with an element size of 128 mm, simulations were performed, and results analyzed. The mesh was refined progressively, reducing the element size consistently across three different resolutions as shown in Figure 3. Surface mesh sizes were 4 mm for the coarsest mesh (Mesh 1) and 1 mm for the finest mesh (Mesh 3), with the total number of elements reaching 2.8 million for Mesh 3. Meanwhile, for all the cases, orthogonal mesh quality was more 0.75. The drag coefficient values exhibited consistent changes as the mesh was refined. The percentage error between Mesh 1 and Mesh 2 was approximately 4%, indicating significant improvement with finer resolution. Further refinement between Mesh 2 and Mesh 3 showed less than 1% error, suggesting minimal impact on results with additional mesh refinement.
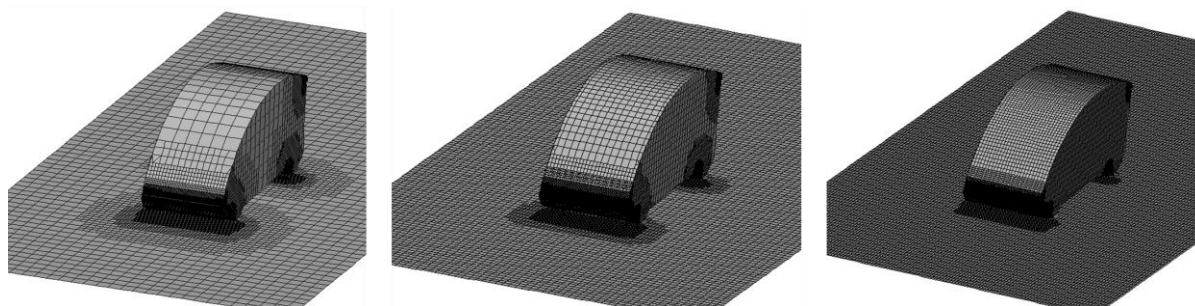

Fig. 3. Three different mesh resolutions; mesh 1, mesh 2 and mesh 3 (from left)

Based on these findings, Mesh 2 was identified as sufficient for predicting aerodynamic loads, as it provided accurate results with minimal computational expense compared to Mesh 3. This approach ensures that the simulation setup is optimized for efficiency while maintaining reliability in predicting the small city vehicle model's aerodynamic performance.

3. Results

3.1 Aerodynamic Forces

In this section, we present a detailed comparison of the aerodynamic force coefficients, specifically drag and lift values calculated at three different velocities: 10 m/s, 15 m/s, and 20 m/s. We evaluate these coefficients using two different turbulence modelling approaches: the traditional RANS (Reynolds-Averaged Navier-Stokes) model and the advanced hybrid RANS/LES (Large Eddy Simulation) or DDES (Delayed Detached Eddy Simulation) turbulence model shown in Figure 4. The RANS model used in this study is the k-ε, which relies on time-averaged Navier-Stokes equations and turbulence closure relationships to predict aerodynamic forces.

The left figure shows the drag coefficients, where RANS results exhibit values of 0.541, 0.539, and 0.538 for speeds of 10, 15, and 20 m/s, respectively. In contrast, the DDES results present slightly lower values of 0.524, 0.518, and 0.514 for the corresponding speeds. This consistent reduction in drag coefficient values from RANS to DDES across all speeds indicates a small difference in turbulence modelling, with DDES showing a reduction of around 3-5% compared to RANS. On the other hand, the right figure displays the lift coefficients, with RANS results remaining relatively stable at 0.129, 0.127, and 0.125 for speeds of 10, 15, and 20 m/s, respectively. However, the DDES results exhibit significantly higher lift coefficients of 0.259, 0.318, and 0.325 for the same speeds, with an increase of up to 150% at the higher speeds compared to RANS. This substantial difference underlines DDES's ability to capture more detailed unsteady flow structures around the vehicle, which significantly impact lift.
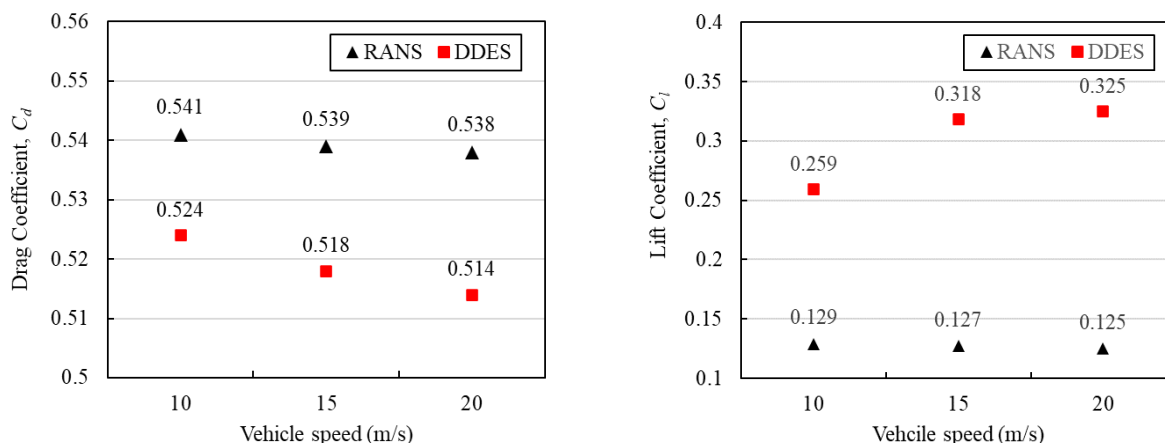

Fig. 4. Drag and lift coefficient at different inlet velocity for RANS and DDES

Studies comparing DDES with RANS and Unsteady RANS have indicated that DDES can predict drag coefficients more accurately, with DDES models showing lower drag coefficients compared to URANS [34,35]. This suggests that DDES is capable of capturing transient vortices and finer turbulence scales that are not adequately resolved by RANS methods, which supports the results from the current study. On the other hand, the higher lift coefficient observed in DDES compared to RANS models can be attributed to the improved accuracy of DES in capturing the flow physics [13].

3.2 Three-Dimensional Vortex Core

Figure 5 shows a series of flow visualizations around a vehicle model for different velocity and turbulence models. The colors represent different velocity magnitudes, with blue indicating lower velocities and red indicating higher velocities. The wake length (L_w) is indicated, representing the distance behind the vehicle where the flow separates and forms a wake. For the RANS model, the L_w is increasing as the inlet velocity increase from 10 m/s to 20 m/s. This provides an initial overview of how the airflow behaves as it passes over and behind the vehicle. Moreover, for all the cases of RANS two pairs of vortices (V_1 and V_2) can be seen around the vehicle. Meanwhile, the frontal edge area of the vehicle with highest velocity are shown.

The RANS simulations display smoother flow fields with fewer small-scale vortices. The turbulence is more uniformly distributed, and the flow appears more attached to the vehicle's surface. Additionally, the RANS method shows less detailed vortex shedding in the wake of the vehicle, resulting in a relatively smooth wake region with less pronounced turbulent structures. The boundary layer appears stable and attached to the surface, particularly around the vehicle's rear. This can contribute to a more predictable aerodynamic force distribution but might underrepresent the actual flow separation and reattachment dynamics.

In contrast, the DDES simulations exhibit a more complex and detailed flow field, with many small-scale vortices and turbulent structures, especially in the wake region. The wake is filled with turbulent eddies and vortices, providing a high level of detail in the flow separation and reattachment zones.
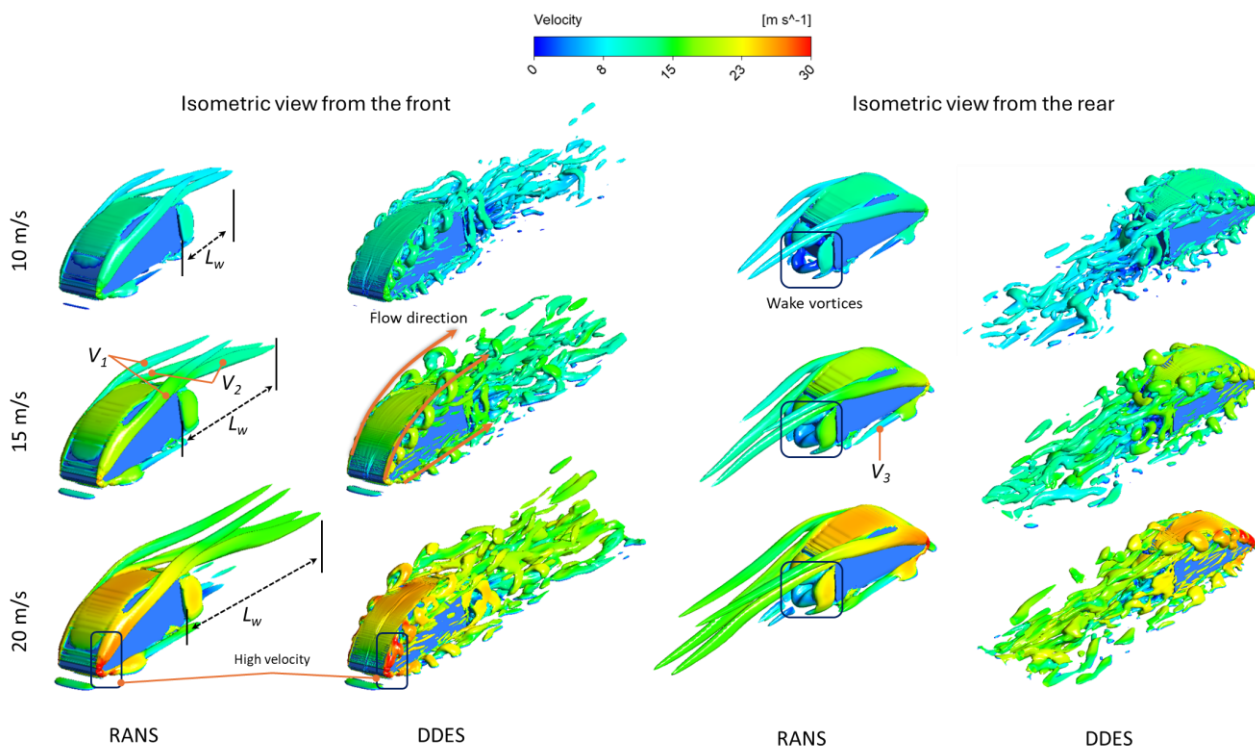

Fig. 5. Iso surface of the Q-criterion, colored with velocity for RANS and DDES

Smoother and more attached flow in RANS results in higher drag coefficients can be seen in Figure 4. Meanwhile, the reduced vortex shedding, and wake turbulence mean that the aerodynamic resistance is higher due to a less efficient pressure recovery in the wake region [36]. On the other hand, detailed vortex shedding, and turbulent wake captured by DDES contribute to lower drag coefficients. The enhanced mixing and turbulence in the wake region facilitate better pressure

recovery, reducing the overall drag on the vehicle. The relatively stable and smooth flow around the vehicle in RANS leads to a more consistent but lower lift coefficient.

3.3 Velocity Characteristics Around the Vehicle

Figure 6 presents a detailed comparison between the RANS and DDES models for flow around a simplified vehicle geometry at plane $x = 0$. It highlights the velocity field in the flow plane and the pressure distribution on the vehicle surface at three different speeds: 10 m/s, 15 m/s, and 20 m/s. Both RANS and DDES simulations illustrate the flow acceleration over the vehicle and deceleration in the wake region. The streamlines in the figure indicate the flow direction and behavior, providing a clear visualization of the aerodynamic performance under different conditions.
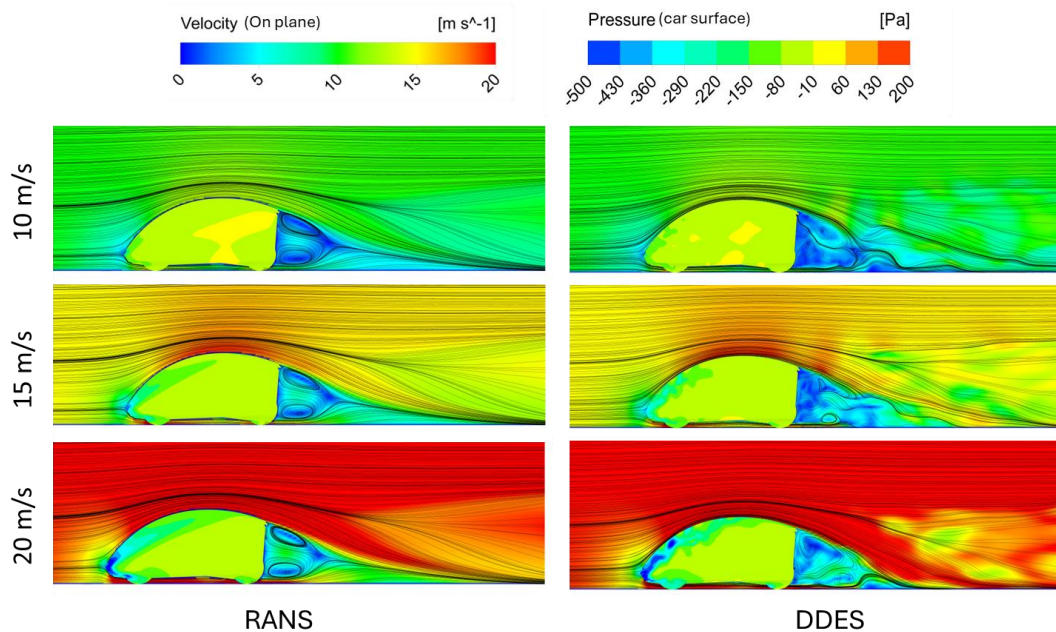

Fig. 6. Comparison of the velocity field in the flow plane, streamlines, and pressure distribution on the vehicle surface for RANS and DDES methods at three different speeds at $x = 0$

At 10 m/s, the RANS flow remains relatively attached to the vehicle's surface, with minimal separation and wake formation. The streamlines show smooth transitions over the vehicle, and the pressure distribution is relatively uniform, featuring higher pressure at the front and lower pressure at the rear, indicating minimal lift and moderate drag. In contrast, the DDES captures more detailed vortices and fluctuations in the wake, indicating a more accurate representation of turbulence. Although the pressure distribution is similar to RANS, there are more localized variations due to better turbulence capture. On the other hand, at 15 m/s, the RANS flow begins to show slight separation near the vehicle's rear, with streamlines indicating a small wake region. There are increased pressure differences, with lower pressure on the roof and higher pressure on the front and rear, suggesting slightly increased drag and lift. The DDES shows detailed separation and vortex formation near the vehicle's rear, with a more complex wake compared to RANS.

At 20 m/s, the RANS flow exhibits more obvious separation and a larger wake region. The streamlines show significant recirculation in the wake, and significant pressure differences are observed, with very low pressure on the roof and high pressure at the rear, contributing to higher drag and reduced lift [37]. The DDES flow shows significant separation with a large, turbulent wake

region. The streamlines depict complex vortex structures and recirculation zones, and the pressure distribution shows significant differences, with very low pressure on the roof and detailed high-pressure regions on the rear and sides, indicating higher lift and lower drag compared to RANS.

To visualize more details flow from the top around the vehicle, two planes are drawn at *y* = -0.2 and *y* = 0.2 in Figure 7 and 8. At *y* = 0.2, both RANS and DDES show similar patterns with slight differences in the wake region behind the vehicle. DDES may show more detailed structures in the wake. The RANS flow field shows a smooth and relatively uniform velocity distribution. Low-velocity regions (blue) are seen directly behind the vehicle, indicating a stable wake and high-velocity regions (green to yellow) are well-developed along the sides of the vehicle. While DDES captures a more detailed and turbulent flow structure. The wake region displays significant velocity fluctuations and eddies, indicating more realistic vortex shedding. Velocity variations are more pronounced compared to RANS, particularly in the wake.

In the analysis of flow configurations at different speeds (10m/s, 15m/s, and 20m/s) using RANS and DDES models, distinct trends emerge. At lower speeds (10m/s), both RANS and DDES show attached flow with minor differences in the wake region, where DDES captures more detailed turbulence. As speed increases to 15m/s, flow separation becomes evident, more pronounced in DDES which depicts complex vortex shedding and turbulent structures compared to RANS, which shows a broader wake with less detail. At higher speeds like 20m/s, RANS struggles to capture complex vortices and turbulent wakes, while DDES excels in representing detailed, fluctuating flow patterns with significant turbulence. Overall, DDES consistently shows superior capability in capturing unsteady flow phenomena and complex turbulent structures compared to the more smoothed-out representations of RANS, particularly evident in higher speed regimes.
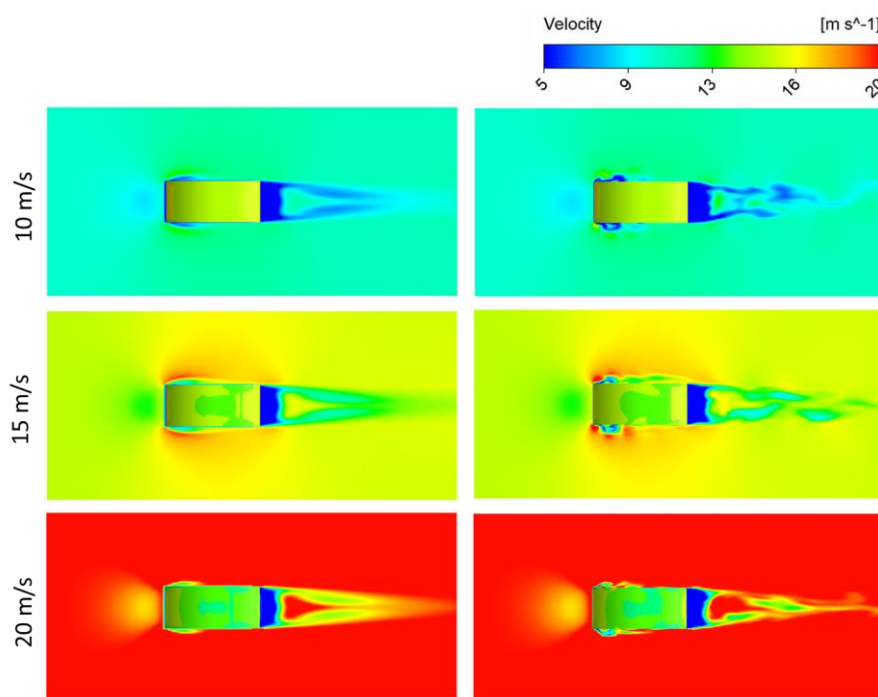

Fig. 7. Comparison of the velocity field on a plane at *y* = 0.2

Additionally, flow structure at lower area of the vehicle presented in Figure 8. In flow condition at 10m/s, both RANS and DDES models show mostly attached flow with a smoother velocity gradient, a stable and smooth flow with limited separation, and a small wake region with low velocity recirculation behind the vehicle. DDES captures minor turbulent structures in the wake, providing more detail than RANS. On the other hand, in velocity speed of 15m/s, flow separation becomes more noticeable. RANS shows a broad but less detailed wake, whereas DDES captures more turbulence and finer structures, with steeper velocity gradients and detailed flow separations and vortices. Furthermore, in flow condition of 20m/s, the wake region and flow separation are more pronounced. RANS struggles to capture detailed vortical structures, while DDES provides a more accurate and detailed representation of the turbulent flow, showing complex eddy formations and increased turbulence in the wake.
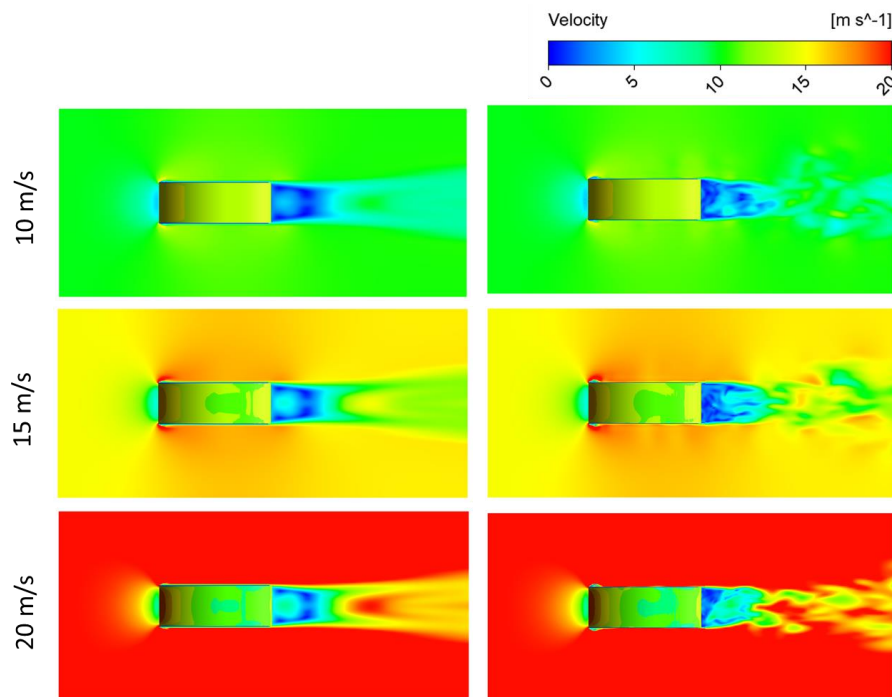

Fig. 8. Comparison of the velocity field on a plane at *y* = -0.2

4. Conclusions

In this study, the aerodynamic performance of a simplified small city vehicle was evaluated under different flow conditions using Reynolds-Averaged Navier-Stokes (RANS) and Delayed Detached Eddy Simulation (DDES) models. The analysis was conducted at three inlet velocities: 10 m/s, 15 m/s, and 20 m/s, focusing on drag and lift coefficients, velocity characteristics, and vortex structures.

At lower speeds (10 m/s), both RANS and DDES show mostly attached flow with smooth velocity gradients and limited wake regions, though DDES captures more detailed turbulent structures. At 15 m/s, flow separation becomes noticeable; RANS shows a broad, less detailed wake, while DDES captures more turbulence and finer structures. At the highest speed (20 m/s), RANS struggles with complex vortical structures and shows smoother flow patterns, whereas DDES accurately represents turbulent flow, revealing complex eddy formations and significant wake turbulence. DDES consistently outperforms RANS in capturing unsteady flow phenomena and complex turbulent structures, especially at higher speeds.

The study underlines the importance of using advanced hybrid models like DDES for accurate aerodynamic predictions, particularly in scenarios involving high Reynolds numbers and significant flow separations. While RANS is effective for general aerodynamic performance predictions, it falls short in capturing detailed unsteady flow structures, which are crucial for precise lift and drag predictions. Therefore, integrating DDES in the design and analysis of small city vehicles can significantly enhance the accuracy of aerodynamic simulations, contributing to the development of more efficient and environmentally friendly urban transport solutions.

Acknowledgement

References

[1] Mądziel, Maksymilian. "Future cities carbon emission models: hybrid vehicle emission modelling for low-emission zones." *Energies* 16, no. 19 (2023): 6928. http://doi.org/10.3390/en16196928

[2] Jiang, Changjun, and Xiaoxuan Liu. "Does high-speed rail operation reduce ecological environment pressure?—Empirical evidence from China." *Sustainability* 14, no. 6 (2022): 3152. http://doi.org/10.3390/su14063152

[3] Russo, Francesco, and Antonio Comi. "Investigating the effects of city logistics measures on the economy of the city." *Sustainability* 12, no. 4 (2020): 1439. http://doi.org/10.3390/su12041439

[4] Jowsey, Lydia, and Martin Passmore. "Experimental study of multiple-channel automotive underbody diffusers." *Proceedings of the Institution of Mechanical Engineers, Part D: Journal of Automobile Engineering* 224, no. 7 (2010): 865-879. http://doi.org/10.1243/09544070JAUTO1339

[5] Dirkx, Dominic, and Erwin Mooij. "Continuous aerodynamic modelling of entry shapes." In *AIAA Atmospheric Flight Mechanics Conference*, p. 6575. 2011. http://doi.org/10.2514/6.2011-6575

[6] Stabile, Pietro, Federico Ballo, Gianpiero Mastinu, and Massimiliano Gobbi. "An ultra-efficient lightweight electric vehicle—Power demand analysis to enable lightweight construction." *Energies* 14, no. 3 (2021): 766. http://doi.org/10.3390/en14030766

[7] Fu, Chen, Mesbah Uddin, and Chunhui Zhang. "Computational analyses of the effects of wind tunnel ground simulation and blockage ratio on the aerodynamic prediction of flow over a passenger vehicle." *Vehicles* 2, no. 2 (2020): 318-341. http://doi.org/10.3390/vehicles2020018

[8] Tsubokura, Makoto, Andrew Kerr, Keiji Onishi, and Yoshimitsu Hashizume. "Vehicle aerodynamics simulation for the next generation on the k computer: part 1 development of the framework for fully unstructured grids using up to 10 billion numerical elements." *SAE International Journal of Passenger Cars-Mechanical Systems* 7, no. 2014-01-0621 (2014): 1106-1118. http://doi.org/10.4271/2014-01-0621

[9] Zhang, Xinfang, Miao Li, Bomin Wang, and Zexian Li. "A Parameter Correction method of CFD based on the Approximate Bayesian Computation technique." In *Journal of Physics: Conference Series*, vol. 2569, no. 1, p. 012076. IOP Publishing, 2023. http://doi.org/10.1088/1742-6596/2569/1/012076

[10] Evans, Ben, Jack Townsend, Oubay Hassan, Kenneth Morgan, Ron Ayers, Mark Chapman, and Andy Green. "On the subsonic and low transonic aerodynamic performance of the land speed record car, Bloodhound LSR." *Proceedings of the Institution of Mechanical Engineers, Part G: Journal of Aerospace Engineering* 236, no. 9 (2022): 1895-1921. http://doi.org/10.1177/09544100211046159

[11] Gilkeson, C. A., V. V. Toropov, H. M. Thompson, M. C. T. Wilson, N. A. Foxley, and P. H. Gaskell. "Dealing with numerical noise in CFD-based design optimization." *Computers & Fluids* 94 (2014): 84-97. http://doi.org/10.1016/j.compfluid.2014.02.004

[12] Abdul-Rahman, H., H. Moria, and Mohammad Rasidi Mohammad Rasani. "Aerodynamic study of three cars in tandem using computational fluid dynamics." *Journal of Mechanical Engineering and Sciences* 15, no. 3 (2021): 8228-8240. http://doi.org/10.15282/15.3.2021.02.0646

[13] Zhang, Chunhui, Charles Patrick Bounds, Lee Foster, and Mesbah Uddin. "Turbulence modeling effects on the CFD predictions of flow over a detailed full-scale sedan vehicle." *Fluids* 4, no. 3 (2019): 148. http://doi.org/10.3390/fluids4030148

[14] Diedrichs, B. "Aerodynamic crosswind stability of a regional train model." *Proceedings of the Institution of Mechanical Engineers, Part F: Journal of Rail and Rapid Transit* 224, no. 6 (2010): 580-591. http://doi.org/10.1243/09544097JRRT346

[15] Felekos, Georgios, Eleni Douvi, and Dionissios Margaris. "Cost-effective numerical analysis of the DrivAer fastback model aerodynamics." *Proceedings of the Institution of Mechanical Engineers, Part D: Journal of Automobile Engineering* 237, no. 14 (2023): 3536-3546. http://doi.org/10.1177/09544070221135908

[16] Islam, M., F. Decker, E. De Villiers, Aea Jackson, J. Gines, T. Grahs, A. Gitt-Gehrke, and J. Comas i Font. *Application of detached-eddy simulation for automotive aerodynamics development*. No. 2009-01-0333. SAE Technical Paper, 2009. http://doi.org/10.4271/2009-01-0333

[17] Li, Tian, Hassan Hemida, Jiye Zhang, Mohammad Rashidi, and Dominic Flynn. "Comparisons of shear stress transport and detached eddy simulations of the flow around trains." *Journal of Fluids Engineering* 140, no. 11 (2018): 111108. http://doi.org/10.1115/1.4040672

[18] Arafat, Mohammad, and Izuan Amin Ishak. "Aerodynamic performance of a next-generation high-speed train under transient crosswind." (2023).

[19] Arafat, Mohammad, Izuan Amin Ishak, Ahmad Faiz Mohammad, Amir Khalid, Md Norrizam Mohmad Jaát, and Mohd Fuad Yasak. "Effect of Reynolds number on the wake of a Next-Generation High-Speed Train using CFD analysis." *CFD Letters* 15, no. 1 (2023): 76-87. http://doi.org/10.37934/cfdl.15.1.7687

[20] Niu, Jiqiang, Yueming Wang, Feng Liu, and Rui Li. "Aerodynamic behavior of a high-speed train with a braking plate mounted in the region of inter-car gap or uniform-car body: A comparative numerical study." *Proceedings of the Institution of Mechanical Engineers, Part F: Journal of Rail and Rapid Transit* 235, no. 7 (2021): 815-826. http://doi.org/10.1177/0954409720965821

[21] Li, Tian, Hassan Hemida, and Jiye Zhang. "Evaluation of SA-DES and SST-DES models using OpenFOAM for calculating the flow around a train subjected to crosswinds." *Proceedings of the Institution of Mechanical Engineers, Part F: Journal of Rail and Rapid Transit* 234, no. 10 (2020): 1346-1357. http://doi.org/10.1177/0954409719895652

[22] Sun, K., Z. Gu, J. Liu, L. Zheng, H. Hu, and J. Gao. "Coupled Analysis of Transient Aerodynamic Characteristics of the Coach under Crosswind in Different Situations." *Journal of Applied Fluid Mechanics* 14, no. 2 (2020): 527-539. http://doi.org/10.47176/jafm.14.02.31703

[23] Boudreau, Matthieu, and Guy Dumas. "Vortex dynamics in the wake of three generic types of freestream turbines." *Journal of Fluids Engineering* 140, no. 2 (2018): 021106. http://doi.org/10.1115/1.4037974

[24] Guilmineau, Emmanuel, G. B. Deng, Alban Leroyer, P. Queutey, Michel Visonneau, and J. Wackers. "Assessment of hybrid RANS-LES formulations for flow simulation around the Ahmed body." *Computers & Fluids* 176 (2018): 302-319. http://doi.org/10.1016/j.compfluid.2017.01.005

[25] Ashton, Neil, Alastair West, Sylvain Lardeau, and Alistair Revell. "Assessment of RANS and DES methods for realistic automotive models." *Computers & fluids* 128 (2016): 1-15. http://doi.org/10.1016/j.compfluid.2016.01.008

[26] Morden, Justin A., Hassan Hemida, and Chris J. Baker. "Comparison of RANS and detached eddy simulation results to wind-tunnel data for the surface pressures upon a class 43 high-speed train." *Journal of Fluids Engineering* 137, no. 4 (2015): 041108. http://doi.org/10.1115/1.4029261

[27] Kamal, Muhammad Nabil Farhan, Izuan Amin Ishak, Nofrizalidris Darlis, Daniel Syafiq Baharol Maji, Safra Liyana Sukiman, Razlin Abd Rashid, and Muhamad Asri Azizul. "A review of aerodynamics influence on various car model geometry through CFD techniques." *Journal of Advanced Research in Fluid Mechanics and Thermal Sciences* 88, no. 1 (2021): 109-125. http://doi.org/10.37934/arfmts.88.1.109125

[28] Pirouz, Behrouz, Domenico Mazzeo, Stefania Anna Palermo, Seyed Navid Naghib, Michele Turco, and Patrizia Piro. "CFD investigation of vehicle's ventilation systems and analysis of ACH in typical airplanes, cars, and buses." *Sustainability* 13, no. 12 (2021): 6799. http://doi.org/10.3390/su13126799

[29] Wu, Chengjun, Jiang Liu, and Jie Pan. "Influence of surrounding structures upon the aerodynamic and acoustic performance of the outdoor unit of a split air-conditioner." *Chinese Journal of Mechanical Engineering* 27, no. 4 (2014): 836-845. http://doi.org/10.3901/CJME.2014.0515.095

[30] Abe, Masato. "Vehicle dynamics and control." *Vehicle Handling Dynamics* (2015): 1-3. http://doi.org/10.1016/B978-1-85617-749-8.00001-5

[31] Favre, Tristan, and Gunilla Efraimsson. "An assessment of detached-eddy simulations of unsteady crosswind aerodynamics of road vehicles." *Flow, Turbulence and Combustion* 87 (2011): 133-163. http://doi.org/10.1007/s10494-011-9333-4

[32] Vasilopoulos, Konstantinos, Ioannis E. Sarris, and Panagiotis Tsoutsanis. "Assessment of air flow distribution and hazardous release dispersion around a single obstacle using Reynolds-averaged Navier-Stokes equations." *Heliyon* 5, no. 4 (2019). http://doi.org/10.1016/j.heliyon.2019.e01482

[33] Chamkha, Ali J., and Younes Menni. "Hydrogen Flow over a Detached V-Shaped Rib in a Rectangular Channel." *Mathematical Modelling of Engineering Problems* 7, no. 2 (2020). http://doi.org/10.18280/mmep.070202

[34] Im, Hongsik, and Gecheng Zha. "Delayed detached eddy simulation of a stall flow over NACA0012 airfoil using high order schemes." In *49th AIAA aerospace sciences meeting including the new horizons forum and aerospace exposition*, p. 1297. 2011. http://doi.org/10.2514/6.2011-1297

[35] Gan, Jiaye, Yiqing Shen, and Gecheng Zha. "Comparison of drag prediction using rans models and ddes for the dlr-f6 configuration using high order schemes." In *54th AIAA Aerospace Sciences Meeting*, p. 0553. 2016. http://doi.org/10.2514/6.2016-0553

[36] Barman, Bhanuman, and Somnath Bhattacharyya. "Control of vortex shedding and drag reduction through dual splitter plates attached to a square cylinder." *Journal of Marine Science and Application* 14 (2015): 138-145. http://doi.org/10.1007/s11804-015-1299-5

[37] Wang, Yiping, Y. Xin, Zh Gu, Sh Wang, Yadong Deng, and Xue Yang. "Numerical and experimental investigations on the aerodynamic characteristic of three typical passenger vehicles." *Journal of Applied Fluid Mechanics* 7, no. 4 (2014): 659-671. http://doi.org/10.36884/jafm.7.04.21460